# A New High Power Factor ZVT-ZCT AC-DC Boost Converter

**Naim Suleyman Ting**[†]

**Abstract** – This paper introduces a new soft switched AC-DC boost converter with power factor correction (PFC). In the introduced converter, all devices are turned on and off under soft switching (SS). The main switch is turned on under zero voltage transition (ZVT) and turned off under zero current transition (ZCT). The main diode is turned on under zero voltage switching (ZVS) and turned off under zero current switching (ZCS). Meanwhile, there is not any current or voltage stress on the main devices. Besides, the auxiliary switch is turned on under ZCS and turned off under ZVS. The detailed theoretical analysis of the converter is presented, and also theoretical analysis is verified by a prototype with 100 kHz and 500 W. Also, the proposed converter has 99.8% power factor and 97.5% total efficiency at soft switching operation.

**Keywords**: Power factor correction, Zero voltage transition, Pulse width modulation, Hard switching, Soft switching.

## 1. Introduction

In recent years, the use of the electrical element is increasing more and more. So, the energy demand is increasing in direct proportion to the energy consumption with advancing technology. Thus, energy usage should be more efficient and economical. Besides, nonlinear power supplies cause impairment the current drawn from grid. For this reason, the high quality energy usage is very important in terms of energy efficiency [1-4]. Power factor correction (PFC) is a demanded feature for AC-DC power supplies. PFC means to near zero reactive power and harmonics essentially. PFC circuits are used between bridge rectifier and output load for eliminating high harmonic content of the line current. The harmonic current causes some issues such as higher total harmonic distortion, poor power factor at input line voltage and current [5-7]. The classical PFC circuits are usually composed two stages. They need to two switches and controllers. So, the cost is higher and the control is more complex in the two stage PFC circuits [8, 9]. For solving these problems, the single-stage PFC converters have been proposed in literature [10-12].

The single-stage PFC circuits have a common switch for regulation and power factor correction. So, their costs are lower and the controls are simpler. PFC circuits should be operated at high frequency in order to reduce harmonic current, increased power density and fast dynamic response. However, their switching losses are increased in high frequency since they usually operate under hard switching (HS) [13-15]. To reduce and/or eliminate the switching losses, soft switching (SS) techniques have been presented in literature [16-32]. SS techniques are zero-voltage-switching (ZVS), zero-voltage-transition (ZVT), zero-

current-switching (ZCS), and zero-current-transition (ZCT). ZVT and ZCT techniques are modern SS techniques and they compose active snubber cells. In these techniques, the switching power losses are eliminated. To reduce the switching losses of MOSFET at turning on, ZVT techniques are preferred; ZCT techniques are preferred to eliminate tailing current losses of IGBT at turning off [16].

In [17, 18], two snubber cells are used to achieve ZVT. So, this case causes to increase the cost. To solve this drawback, some passive snubber cells are proposed in [19-21]. So, the cost is reduced since the auxiliary switch has not been used in the passive snubber cells. But, the converter in [19] is not suitable for PFC applications because of frequency modulation usage. In [20, 21], there are the extra voltage and current stress across the switches.

In [22, 23], the switches operate under HS. So, the switching power losses cannot be reduced. In [24], although the main switches are turned on under ZVT without additional current or voltage stress, the auxiliary switch has been operated with HS. Thus, the switching power losses of snubber cell are fairly high. In [25], the main switches are turned on with ZVT and the auxiliary switch is turned off with ZCS. But, the number of components in the circuit is more. So, the cost of the converter is increased. In [26], the design and implementation of converter is difficult since the coupled inductor is used in the snubber cell. Additionally, the leakage inductance losses cause to decrease the efficiency of converter.

In [27], these switches do not have common ground and this case causes difficulty of application. In [28], the main switches are operated with SS but there are the extra current and voltage stress across the main switches. For this reason, the conduction losses of the switches are increased. In [29, 30], all devices are turned on and off with SS without additional current or voltage stresses. However, the auxiliary resonance inductors are on the

† Corresponding Author: Dept. of Electrical-Electronic Engineering, Erzincan University, Turkey. (nsuleyman@erzincan.edu.tr)

path that the main current flows. So, the cost and weight of converter is increased. Also, this case causes the oscillations between the resonance inductors and the parasitic capacitances of the switches.

In this paper, a new ZVT-ZCT PWM AC-DC PFC boost converter is introduced. In the proposed converter, the main switch is turned on under ZVT and is turned off under ZCT as well as the main diode is turned on under ZVS and is turned off under ZCS without the extra current or voltage stress. Also, the auxiliary switch is turned on under ZCS and turned off under ZVS. The proposed converter eliminates the switching power losses compared classical PFC boost converter. The aim of the presented converter is to reduce the switching losses and achieve the high efficiency and unity power factor at high frequency operation. The basic circuit scheme of the proposed ZVT-ZCT AC-DC PFC boost converter is shown in Fig. 1. Additionally, this new snubber cell has been presented with simulation results by me in a conference. Conference paper is given in ref. [31]. Besides, my conference paper is extended and improved by me. This paper presents my conference paper's extended version with mathematical analysis, experimental results, the efficiency analysis etc. in detail.

## 2. Operation Modes of Proposed Converter

In the presented AC-DC PFC boost converter shown in Fig. 1., $V_i$ is AC input voltage source, $S_1$ is main switch, $L_F$ is main inductor, $C_F$ is output capacitor, $D_F$ is main diode, $S_2$ is auxiliary switch, $L_a$ and $L_b$ are resonance inductors, $D_2$ is auxiliary diode, $C_s$ is resonance capacitor and $C_p$ is the sum of the parasitic capacitors.

The following assumptions are made to facilitate theoretical analysis.
- $C_F$ is large enough because the output voltage can be kept constant.
- $L_F$ is assumed large enough to keep input current constant.
- The reverse recovery currents of diodes are neglected.

There are eleven operation modes in a switching cycle. The equivalent circuits of operation modes are shown in Fig. 2. The key waveforms of the operation modes are shown in Fig. 3.

**Mode 1** [$t_0 < t < t_1$: Fig. 2 (a) ]
Before this mode, the switches are in off-state. At t = $t_0$,
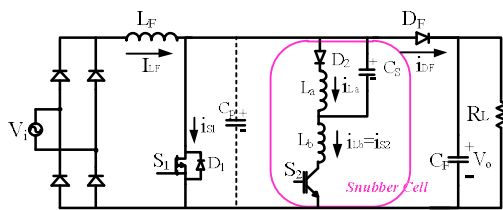


**Fig. 1.** The basic circuit scheme of the proposed converter

$i_{S1} = 0$, $i_{DF} = I_{LF}$, $i_{S2} = i_{Lb} = 0$, $i_{La} = 0$, $v_{Cp} = V_o$ and $v_{Cs} = -V_{C0}$ are valid. In here, $I_{LF}$ is the current of main inductor, $v_{Cp}$ is the voltage of $C_p$ parasitic capacitor, $v_{Cs}$ is the voltage of $C_s$ snubber capacitor and $V_{Co}$ is the initial voltage value of the $C_s$ snubber capacitor. After a PWM control signal is applied to auxiliary switch, the current of the main diode decreases. Also, the current of auxiliary switch and the voltage of $C_s$ capacitor increase. The current of lower resonant inductance $i_{Lb}$ and the voltage of resonant capacitance $v_{cs}$ are

$$i_{Lb} = \frac{V_o + V_{Co}}{\omega_1 L_b} sin(\omega_1(t - t_0)) \tag{1}$$

$$v_{Cs} = V_{C0} cos(\omega_1(t - t_0)) \tag{2}$$

where

$$\omega_1 = \sqrt{\frac{1}{L_b C_s}} \tag{3}$$

At the end of this mode, the current of main diode falls zero and the current of $L_b$ reaches input current level. Also, the voltage of the snubber capacitor reaches $-V_{C1}$ value. Thus, the auxiliary switch is turned on under ZCS and the main diode is turned off under ZCS. $V_{C1}$ is the voltage value across the $C_s$ snubber capacitor at the end of Mode 1.

**Mode 2** [$t_1 < t < t_2$ : Fig. 2 (b) ]
At t = $t_1$, $i_{S1} = 0$, $i_{DF} = 0$, $i_{S2} = i_{Lb} = I_{LF}$, $i_{La} = 0$, $v_{Cp} = V_o$ and $v_{Cs} = -V_{C1}$ are valid. In this mode, the energy of $C_p$ is transferred to snubber cell by a resonance beginning between $C_p$ and the snubber cell. So, the voltage of $C_P$ decreases while $i_{Lb}$ current and the voltage of $C_s$ are increasing. For this mode, the current of lower resonant inductance $i_{Lb}$ and the voltage of snubber capacitance $v_{cp}$ are

$$i_{Lb} = I_i + \frac{V_o + V_{C1}}{\omega_2 L_b} sin(\omega_2(t - t_1)) \tag{4}$$

$$v_{Cp} = (V_0 + V_{C1}) cos(\omega_2(t - t_1)) - V_{C1} \tag{5}$$

where

$$\omega_2 = \sqrt{\frac{1}{L_b(C_p + C_s)}} \tag{6}$$

At the end of this mode, the voltage of $C_p$ falls zero and $i_{Lb}$ current reaches the maximum value. Also, the voltage of $C_s$ is equal to zero.

**Mode 3** [$t_2 < t < t_4$ : Fig. 2(c)]
In this mode, a new resonance starts via $L_b - L_a - C_s$ and the energy of $L_b$ is transferred to $L_a$ and $C_s$ through internal diode of the main switch. This mode is called ZVT interval. In this mode, a PWM control signal is applied to the main

**Fig. 2.** Equivalent circuit schemes of the operation modes in the proposed boost converter. (a) Mode 1, (b) Mode 2, (c) Mode 3, (d) Mode 4, (e) Mode 5, (f) Mode 6, (g) Mode 7, (h) Mode 8, (i) Mode 9, (j) Mode 10, (k) Mode 11

switch; so the main switch is turned on under ZVT.

At t = t$_3$, the current of L$_b$ falls the input current level and D$_1$ diode is turned off under ZCS. Later, the current of the main switch increases; the current of inductance L$_b$ continues to decrease. For this mode, the currents of lower and upper resonant inductances i$_{Lb}$, i$_{La}$ and the voltage of resonant capacitance v$_{cs}$ are

$$i_{La} = \frac{L_e}{L_a} I_{Lb2} \left(1 - cos\left(\omega_3 \left(t - t_2\right)\right)\right) \qquad (7)$$

$$i_{Lb} = \frac{L_e}{L_a} I_{Lb2} \left(1 - cos\left(\omega_3 \left(t - t_2\right)\right)\right) + I_{Lb2} cos\left(\omega_3 \left(t - t_2\right)\right) \qquad (8)$$

$$v_{Cs} = Z_1 \left(I_{Lb2} - I_{La3}\right) sin\left(\omega_3 \left(t - t_2\right)\right) \qquad (9)$$

where

$$Z_1 = \sqrt{\frac{L_e}{C_s}} \qquad (10)$$

$$\omega_3 = \sqrt{\frac{1}{L_e C_s}} \qquad (11)$$

$$L_e = \frac{L_a L_b}{L_a + L_b} \qquad (12)$$

**Mode 4** [t$_4$ < t < t$_5$ : Fig. 2(d) ]

At the beginning of this mode, the current of main switch reaches the input current level and the auxiliary switch is turned off under ZCS because its current falls to zero. During this mode, the energy stored in upper snubber inductance L$_a$ is transferred to capacitor C$_s$ via resonance. For this mode, the current of upper resonant inductance i$_{La}$

and the voltage of resonant capacitance $v_{cs}$ are

$$i_{La} = I_{La4} cos\left(\omega_4 \left(t - t_4\right)\right) + \frac{V_{C4}}{Z_2} sin(\omega_4(t - t_4)) \qquad (13)$$

$$v_{Cs} = V_{C4} cos\left(\omega_4 \left(t - t_4\right)\right) + Z_2 I_{La4} sin(\omega_4(t - t_4)) \qquad (14)$$

where

$$Z_2 = \sqrt{\frac{L_a}{C_s}} \qquad (15)$$

$$\omega_4 = \sqrt{\frac{1}{L_a C_s}} \qquad (16)$$

At the end of this mode, the voltage of capacitor $C_s$ reaches to maximum voltage value in adverse direction and the current of the snubber inductor $L_a$ falls to zero.

**Mode 5** [$t_5 < t < t_6$ : Fig. 2(e) ]
This mode is on-mode of classical boost converter. This mode ends when a PWM control signal is applied to the auxiliary switch.

**Mode 6** [$t_6 < t < t_8$: Fig. 2(f) ]
At the beginning of this mode, a PWM control signal is applied to the auxiliary switch and it is turned on under ZCS owing to inductance $L_b$. Then, a resonance starts between the snubber capacitor $C_s$ and the snubber inductance $L_b$. The current of the main switch begins to decrease while the current of snubber inductance $L_b$ is increasing.

At $t = t_7$, the current of main switch falls to zero when the current of $L_b$ reaches the level of input current. The internal diode of main switch conducts the excess of input current. This mode is called ZCT interval where $D_1$ is at on-state. The control signal of the main switch is removed when its internal diode is in on-state. Thus, the main switch turns off under ZCT. For this mode, the current of lower resonant inductance $i_{La}$ and the voltage of resonant capacitance $v_{cs}$ are

$$i_{Lb} = i_{S2} = \frac{V_{Csmax}}{Z_3} sin\left(\omega_1 \left(t - t_6\right)\right) \qquad (17)$$

$$v_{Cs} = V_{Csmax} cos\left(\omega_1 \left(t - t_6\right)\right) \qquad (18)$$

where

$$Z_3 = \sqrt{\frac{L_b}{C_s}} \qquad (19)$$

At the end of this mode, the current of $L_b$ reaches the maximum value when the voltage of snubber capacitor $C_s$ falls to zero.

**Mode 7** [$t_8 < t < t_9$ : Fig. 2(g) ]
In this mode, a new resonance starts via $L_b - L_a - C_s$. So,

the energy of the $L_b$ is transferred to $L_a$ and $C_s$. Then, the voltage of $C_s$ begins to become positive and the current of $L_a$ begins to increase. For this mode, the currents of lower and upper resonant inductances $i_{Lb}$, $i_{La}$ and the voltage of resonant capacitance $v_{cs}$ can be expressed as follows:

$$i_{La} = \frac{L_e}{L_a} I_{Lbmax} \left(1 - cos\left(\omega_3 \left(t - t_8\right)\right)\right) \qquad (20)$$

$$i_{Lb} = \frac{L_e}{L_a} I_{Lbmax} \left(1 - cos\left(\omega_3 \left(t - t_8\right)\right)\right)$$
$$+ I_{Lbmax} \left(1 - cos\left(\omega_3 \left(t - t_8\right)\right)\right) \qquad (21)$$

$$v_{Cs} = \frac{I_{Lbmax}}{\omega_3 C_s} sin\left(\omega_3 \left(t - t_8\right)\right) \qquad (22)$$

At $t = t_9$, $D_1$ is turned off after the current of $L_b$ falls to the input current level and this mode ends.

**Mode 8** [$t_9 < t < t_{10}$ : Fig. 2(h) ]
In this mode, a resonance occurs via $C_p - L_a - L_b - C_s$ under the constant input current. So, the current of the $L_a$ and the voltage of the $C_s$ increase while the current of $L_b$ is decreasing. In this mode, the following equations are written:

$$L_a \frac{di_{La}}{dt} = v_{Cs} \qquad (23)$$

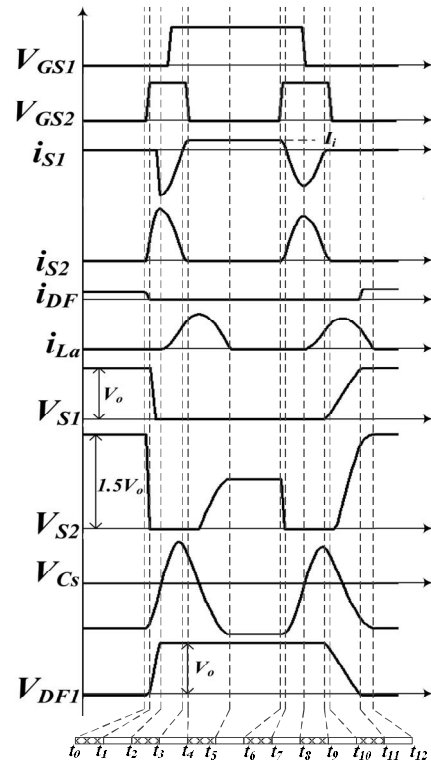$$L_b \frac{di_{Lb}}{dt} = v_{Cp} - v_{Cs} \qquad (24)$$



**Fig. 3.** The key waveforms concerning the operation modes of the proposed boost converter

$$C_s \frac{dv_{Cs}}{dt} = i_{Lb} - i_{La} \qquad (25)$$

$$C_p \frac{dv_{Cp}}{dt} = I_i - i_{Lb} \qquad (26)$$

At t = $t_{10}$, the current of $L_b$ falls to zero and the control signal of auxiliary switch is removed. So, it is turned off under ZCS.

**Mode 9** [$t_{10} < t < t_{11}$ : Fig. 2(i) ]

In this mode, the parasitic capacitor $C_p$ is linearly charged under the constant input current and the energy stored in the $L_a$ is transferred to the $C_s$ via $L_a$ - $D_2$ - $C_s$ resonance. For this mode, the current of upper resonant inductance $i_{La}$ and the voltage of resonant capacitances $v_{cs}$ and $v_{cp}$ can be expressed as follows:

$$i_{La} = I_{La10}cos\left(\omega_4\left(t - t_{10}\right)\right) + \frac{V_{Cs10}}{Z_2}sin(\omega_4(t - t_{10})) \qquad (27)$$

$$v_{Cs} = V_{Cs10}cos\left(\omega_4\left(t - t_{10}\right)\right) - Z_2 I_{La10}sin(\omega_4(t - t_{10})) \qquad (28)$$

$$v_{Cp} = \frac{I_i}{C_p}(t - t_{10}) \qquad (29)$$

At t = $t_{11}$, the main diode is turned on under ZVS when the voltage of $C_p$ reaches the output voltage.

**Mode 10** [$t_{11} < t < t_{12}$ : Fig. 2 (j) ]

During this mode, the resonance between $L_a$ and $C_s$ goes on. For this mode, the current of upper resonant inductance $i_{La}$ and the voltage of resonant capacitance $v_{cs}$ can be expressed as follows:

$$i_{La} = I_{La11}cos\left(\omega_4\left(t - t_{11}\right)\right) - \frac{V_{C11}}{Z_2}sin(\omega_4(t - t_{11})) \qquad (30)$$

$$v_{Cs} = -V_{C11}cos\left(\omega_4\left(t - t_{11}\right)\right) + Z_2 I_{La11}sin(\omega_4(t - t_{11})) \qquad (31)$$

At t = $t_{12}$, the current of $L_a$ falls to zero and the voltage of $C_s$ reaches -$V_{C0}$ value. So, this mode is finished.

**Mode 11** [$t_{12} < t < t_{13}$ : Fig. 2 (k) ]

This mode is off-mode of classical boost converter. During this mode, the input current is transferred to the output through the main diode. When a control signal to the auxiliary switch, it is returned to initial conditions and the modes expressed is repeated in the next switching cycle.

## 3. Design Procedure and Soft Switching Conditions

In this section, the design considerations and the soft switching conditions of the presented converter are explained. The experimental circuit parameters of the presented converter are given in Table I. An example of

ZVT-ZCT PWM boost PFC converter is designed and realized. Its specifications are listed below:

- Input AC voltage: $v_i(t) = 200 \sin(2\pi \times 50t)$.
- Output DC voltage: $V_o = 400$ V.
- Maximum output power: $P_{o, max} = 500$ W.
- Switching frequency: $f_s = 100$ kHz

Be sure that the symbols used in your equation have been defined before the equation appears or immediately following.

### 3.1 Design curves

The characteristic curves of the proposed PFC boost converter are shown in between Fig. 4 and Fig. 7. These curves will be considered when the elements of converter are determined. In these curves, the value of snubber inductance $L_b$ is kept constant at 3 µH and the variations of $L_a$ and $C_s$ are graphically shown. In the figures, $L_a$ is changed between 4µH and 8 µH when $C_s$ is changed between 3 nF and 8 nF. So, the optimum values for $L_a$ and $C_s$ are determined from these figures.

As shown in Fig. 4, the duration of ZVT increases while the value of $L_a$ is decreasing and the value of $C_s$ is increasing. Fig. 5 illustrates that the duration of ZCT is constant while the value of $L_a$ is increasing. On the other hand, the duration of ZCT increases when the value of $C_s$ increases.

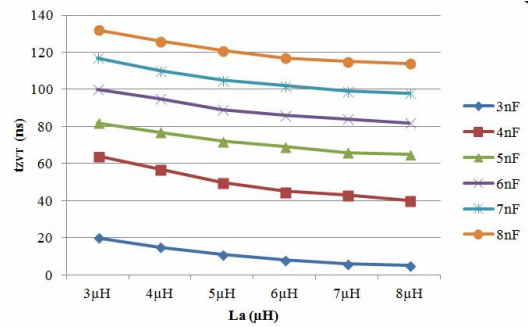In Fig. 6, as expressed in fourth interval, it is shown that



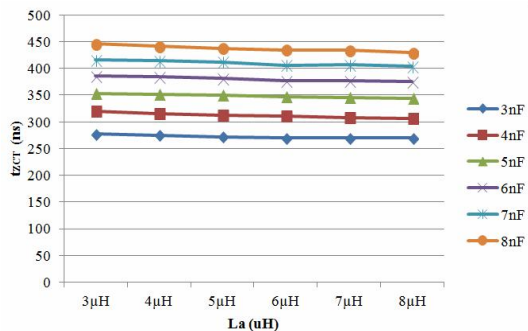**Fig. 4.** The variation of main switch ZVT duration depending on $L_a$ - $C_s$.



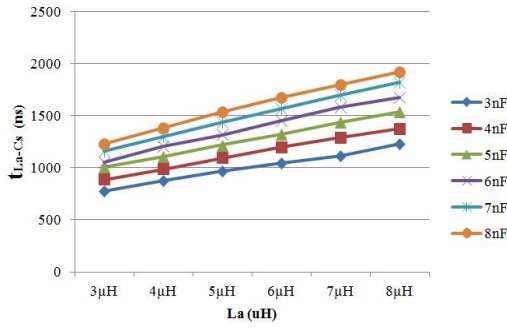**Fig. 5.** The variation of main switch ZCT duration depending on $L_a$ - $C_s$.

**Fig. 6.** The variation of resonance duration between $L_a$ - $C_s$
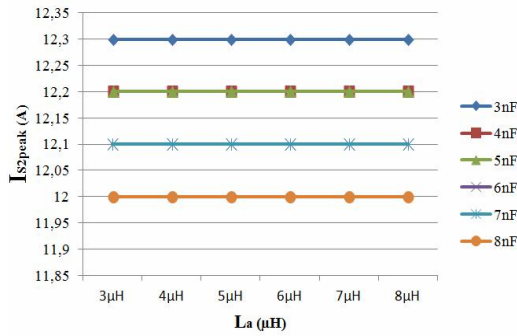


**Fig. 7.** The variation of the auxiliary switch peak current depending on $L_a$ - $C_s$

the variations of resonance duration between $L_a$ and $C_s$. This duration is more important because it affects to total time of resonance between Mode 8 and Mode 10. It is possible to see from curves that $t_{La-Cs}$ duration increases depending on increasing of the values $L_a$ and $C_s$. $t_{La-Cs}$ is resonance duration between $L_a$ and $C_s$.

Finally, Fig. 7 illustrates the variation of resonance peak current that the auxiliary switch $S_2$ conducts. This peak value is fairly important in order to be provided ZVT and ZCT conditionals. It is shown from curves that the variation of $L_a$ does not change the peak current of $S_2$ but the decreasing of $C_s$ is increased the peak value of this current. As shown in figure, the resonance current reaches to twice of the input current.

### 3.2 Design procedure

The main inductor is selected from the following equation:

$$\Delta I_L = D(1-D)\frac{V_o}{f_s L} \qquad (32)$$

where D is the duty cycle of the main switch's control signal. Also, the ripple of boost inductor is accepted by $\Delta I_L\% = 20\%$. In this case; the value of main inductor is selected by 1 mH from Eq. (32).

The main capacitor is selected from the following equation:

$$\Delta V_C = \frac{DI_o}{f_s C} \qquad (33)$$

where the ripple of output capacitor is accepted by $\Delta V_C\% = 1\%$. In this case; the value of output capacitor is selected by 470 µF from Eq. (33).

The parasitic capacitor $C_p$ consists of sum of the parasitic capacitor of main switch, diode and the other parasitic capacitors. This value is almost 1- 2 nF. Therefore, it does not require an extra capacitor. The snubber inductance $L_b$ must choose to provide ZCS at turning-on for auxiliary switch $S_2$. It is considered the turning-on duration $t_r$ of $S_2$ to be determined this value.

$$\frac{V_o}{L_b}t_r \le I_{imax} \qquad (34)$$

At the same time, the value of snubber inductance $L_a$ should be at least twice as bigger than $L_b$ because the auxiliary switch $S_2$ is turned off under ZCS.

$$L_a \ge 2L \qquad (35)$$

In this case, the value of snubber inductance $L_b$ is chosen 3 µH then La is 6 µH.

As a shown in Fig. 4 and Fig. 5, a smaller snubber capacitor means to less ZCT and ZVT durations. Less ZVT and ZCT durations are undesirable. If the value of $C_s$ is increased, ZVT and ZCT durations increase. But in this case, the resonance duration between $L_a$ - $C_s$ and the other resonance durations will be extend. Consequently, the transient resonance intervals increase in a period and an undesirable case occurs. Because the total transient resonance intervals should be less than 20% of total time of a period in order to assure PWM operation. For this reason, the value of $C_s$ cannot be increased over a determined value. Finally, the peak value of resonance current should be twice of the peak value of main inductance current because the soft switching should be ensure even in the worst conditions that the input current has maximum value. The Fig. 7 can be used for determining this current value. It is seen that the most suitable value for $C_s$ is 4.7 nF.

### 3.3 Soft switching conditions of proposed converter

For ZVT and ZCT durations, the necessary values of inductances and capacitors are determined from simulation operation as showing in Fig. 4 - Fig. 7 of paper. If the sum of the transient intervals is $t_{resonant}$ duration, the minimum and maximum durations of the turning-on signal of the main switch should be as following:

$$T_{on-min} \ge t_{resonant} \qquad (36)$$

$$T_{on-max} \le T_p - t_{resonant} \qquad (37)$$

where $t_{resonant}$ is the resonant period and $T_p$ is the switching cycle. Also, if the sum of the transient intervals is allowed to be equal to at most 20% of the switching cycle, for possible the switching period should be as following:

$$T_p = 5 \cdot t_{resonant} \qquad (38)$$

In this case, for the minimum and maximum values of the duty ratio in the converter by using (36) and (37)

$$D_{min} = \frac{T_{on-min}}{T_p} = \frac{t_{resonant}}{5 \cdot t_{resonant}} = 0.2 \qquad (39)$$

$$D_{max} = \frac{T_{on-max}}{T_p} = \frac{4 \cdot t_{resonant}}{5 \cdot t_{resonant}} = 0.8 \qquad (40)$$

are achieved. A lower operation frequency selected results in a smaller minimum and a larger maximum duty ratio.

## 4. Experimental Results

A prototype of the presented PFC converter is realized at 500 W and 100 kHz and it is verified the predicted analysis of the converter. In the experimental prototype, the value of output capacitor is 470 μF, the values of main inductors are 1 mH and the values of resonance inductors are 6 μH and 3 μH. The value of resonance capacitor is 4.7 nF. To obtain the control signals of the switches, the control circuit associated with the UC3854 integrated circuit is designed in the PFC converter as suggested in [33]. The control circuit is given in Fig. 8 in which the input current, voltage and output voltage are sensed. Then, UC3854 generates the gate pulses for the switch with appropriate duty cycle. The PWM controller has low bandwidth such that the duty cycle remains almost constant in order to keep the input current harmonics low. So, the power factor is improved. UC3854 integrated circuit generates the control signal of the boost switch. The auxiliary switch control signal is produced by using the control signal of the boost switch with the help of the analog card. IXGR50N60C2D1 switch is preferred as the main switch and BUP 203 switch is
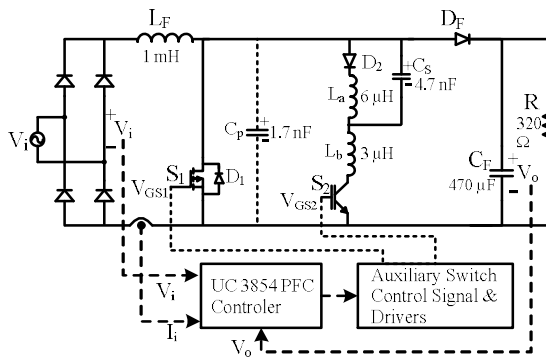
preferred as the auxiliary switch. Also, MUR860 diode is used as the main diode and DESI8-06 diode is used as the
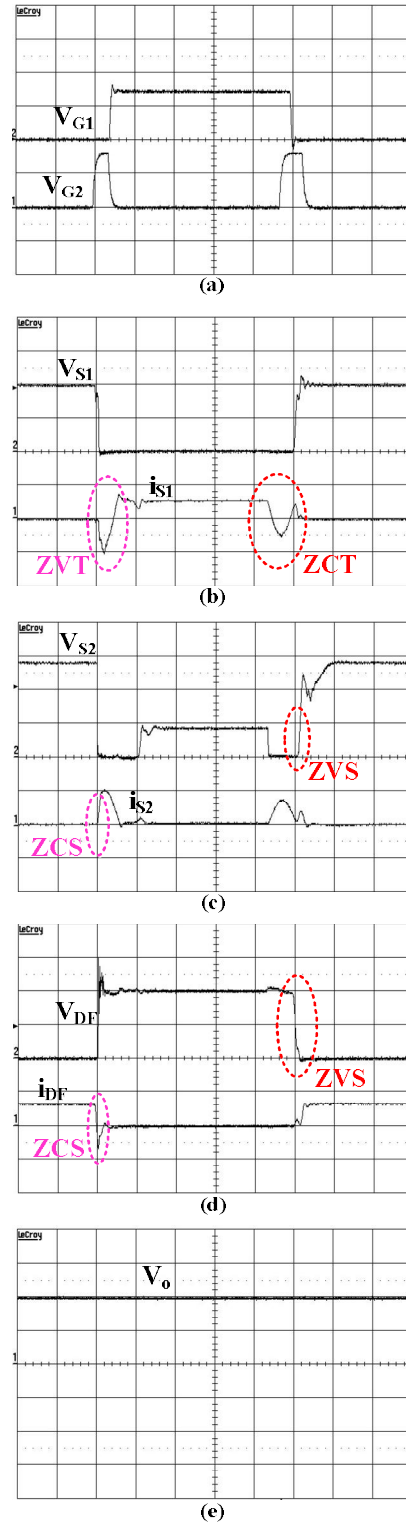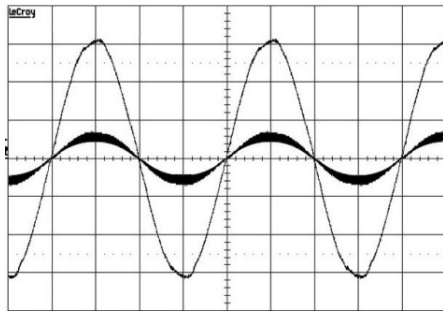


**Fig. 9.** Experimental results (a) Control signals of the switches (10 V/div and 1 μs/div), Voltages and currents of (b) Main switch, (c) Auxiliary switch, (d) Main diode (200 V/div, 5 A/div and 1 μs/div), (e) Output voltage (200 V/div and 5 μs/div)



**Fig. 8.** Control circuit of the proposed converter

**Table 1.** Part number and nominal values of the elements used in experimental circuit

| Element | Part Number | V (V) | I (A) | $t_r$ (ns) | $t_f$ (ns) | $t_{rr}$ (ns) |
|---------|-------------|-------|-------|-----------|-----------|---------------|
| $S_1$ | IXGR50N60C2D1 | 600 | 40 | 45 | 40 | 140 |
| $S_2$ | BUP 203 | 1000 | 23 | 30 | 20 | - |
| $D_F$ | MUR860 | 600 | 8 | - | - | 60 |
| $D_2$ | DESI8-06 | 600 | 8 | - | - | 50 |

**Table 2.** The switching of elements in the converter

| Device | Turning on | Turning off |
|--------|-----------|-------------|
| *Main Switch $S_1$* | ZVT | ZCT |
| *Main Diode $D_F$* | ZVS | ZCS |
| *Auxiliary Switch $S_2$* | ZCS | ZVS |
| *Auxiliary Diode $D_2$* | ZCS | ZVS |



**Fig. 10.** Current and voltage of ac input line (100 V/div, 5 A/div and 5 ms/div)



**Fig. 11.** Efficiency graphics of the proposed converter in case of SS and HS



**Fig. 12.** The power factor graphic of the proposed converter depending on output power

auxiliary diode. The part numbers and some major nominal values of the semiconductor devices used in the presented converter are given in Table 1.

Fig. 9 shows the experimental results of the proposed PFC boost converter taken at nominal load. These results verify the previously mentioned theoretical analysis. In Fig. 9 (a), PWM control signals of the switches are shown. In Fig. 9 (b), the current and voltage of the main switch are shown. As shown in figure, the voltage of main switch is fallen to zero with the snubber cell before the main switch is turned on. Then, the main switch is turned on under ZVT while the internal diode of main switch conducts. Likewise, the current of main switch is fallen to zero the snubber cell before the main switch is turned off. Then, the main switch is turned off under ZCT while the body diode of main switch conducts. Also, it can be seen that there is not any voltage or current stress across main switch.

In Fig. 9 (c), the current and voltage of auxiliary switch are shown. As shown in figure, the auxiliary switch is turned on under ZCS and turned off under ZVS. Additionally, it can be seen from results that the value of voltage stress across auxiliary switch is equal to 1.5Vo.

In Fig. 9 (d), the current and voltage of main diode obtained from experimental results are given. As shown in figure, the main diode is turned on under ZVS and turned off under ZCS without any current or voltage stress. In Fig. 9 (e), the output voltage waveform is given. As shown in figure, the output voltage is constant at 400 V.

The input voltage and current are given in Fig. 10. It is clear that the power factor is near unity with 0.99 value. Also, the current waveform shows that the presented PFC converter operates in continuous conduction mode (CCM). The current and voltage waveform of AC input has sinusoidal shape.
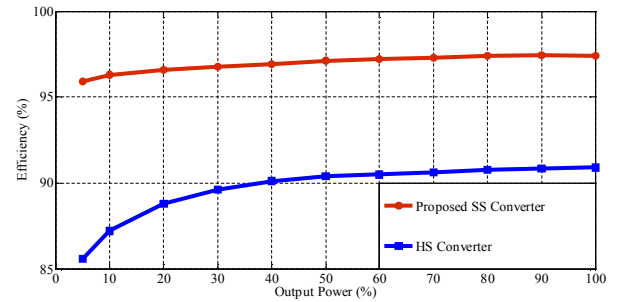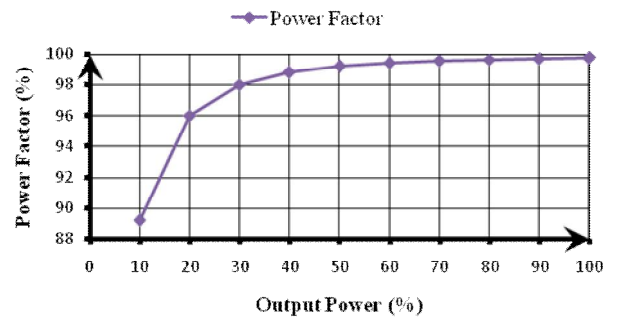
The efficiency graphics of the presented PFC converter for soft switching and hard switching are shown in Fig. 11. While the efficiency value of converter is 91% by hard switching, it is measured about 97.5% for soft switching at the nominal output power. Finally, the experimental measured power factor is 99.8% and THD is 6.4% at full load. Besides, the variation of PF depending on loads is shown given in Fig. 12. As show in figure, when the output power is increased, PF is increased.

Consequently, all devices are turned on and turned off under SS. Any extra current or voltage stress does not occur across the main devices. The SS operation of the proposed converter is maintained for wide load ranges. The results obtained by regarding the switching of devices are mentioned in Table 2.

In the proposed converter, the type of load used is resistive load. The best way to increase the power factor is to reduce the phase difference between the input current and the input voltage. To accomplish PFC, a control is made based on the feedback of the input current. Firstly, the inductance current is sensed and it is passed through the current error amplifier. Then, the control signal of the

semi conductor switch is generated accordingly. So that the difference between the sinusoidal reference current and the average input current is minimized. Also, the value of filter inductance should be reduced. However, the decreasing the filter inductance depends on increasing the switching frequency. As a result, the switching frequency should be increased to increase the power factor in the proposed converter. Soft switching techniques are necessary at high frequency since increasing the switching frequency leads to the switching power losses. So, both PFC and SS in the new converter are realized with a control circuit.

The features of the proposed ZCZVT - PWM boost converter can be summarized as follows.

1) The main switch is turned on under ZVT and turned off under ZCT. The main diode is turned on under ZVS and turned off under ZCS. The auxiliary switch is turned on and turned off under ZCS. Additionally, the other auxiliary semiconductor elements operate under soft switching.

2) The extra current or voltage stress does not occur on the main switch and diode.

3) The proposed converter operates under soft switching for the overall load ranges. The snubber cell assures ZVT turning-on and ZCT turning-off under the light loads.

4) The transient intervals compose a little part of period and the circulation energy is very low.

5) The control of the converter is easy since the auxiliary and main switches have a common ground.

This converter includes both ZVT and ZCT techniques in a cell using quite a few elements because of that it is cheap and simple compared to previous studies.

## 5. Conclusion

In this study, a new PFC boost converter with active snubber cell is presented. Owing to the presented snubber cell, the main switch is turned on under ZVT and turned off under ZCT by lossless. Also, it provides that the main diode is turned on under ZVS and turned off under ZCS. Thus, it minimizes the reverse recovery losses of the main diode. Also, it does not compose any extra voltage or current stress on the main devices. Besides, the auxiliary switch and diode operate under SS and so, they are turned on under ZCS and turned off under ZVS. The power factor of the new converter has been measured as 99.8%. Additionally, total efficiency of converter is reached approximately 97.5% at nominal output power.

## References

[1] Haci Bodur and Suat Yildirmaz, "A New ZVT Snubber Cell for PWM-PFC Boost Converter," *IEEE Trans. Ind. Electron.*, vol. 64, no. 1, pp. 300-309, Jan. 2017.

[2] Sin-Woo Lee and Hyun-Lark Do, "Soft-Switching Two-Switch Resonant AC–DC Converter with High Power Factor," *IEEE Trans. Ind. Electron.*, vol. 63, no. 4, pp. 2083−2091, Apr. 2016.

[3] Cong-Long Nguyen, Hong-Hee Lee and Tae-Won Chun, "A Simple Grid-Voltage-Sensorless Control Scheme for PFC Boost Converters," *Journal of Power Electron.*, vol. 14, no. 4, pp. 712-721, Jul. 2014.

[4] Chih-Chiang Hua, Yi-Hsiung. Fang and Chin-Hsiung Huang, "Zero-Voltage-Transition Bridgeless Power Factor Correction Rectifier with Soft-Switched Auxiliary Circuit," *IET Power Electron.*, vol. 9, no. 3, pp. 546−552, Mar. 2016.

[5] Chung-Ming. Young, Sheng-Feng Wu, Ming-Hui Chen and Sing-Jhao Chen, "Single-Phase AC to High-Voltage DC Converter with Soft-Switching and Diode-Capacitor Voltage Multiplier," *IET Power Electron.*, vol. 7, no. 7, pp. 1704-1713, Jul. 2014.

[6] Amin Emrani, Mohammad Mahdavi and Ehsan Adib, "Soft Switching Bridgeless PFC Buck Converters," *Journal of Power Electron.*, vol. 12, no. 2, pp. 268-275, Mar. 2012.

[7] Khariul Safuan Bin Muhammad and Dylan Dah-Chuan Lu, "ZCS Bridgeless Boost PFC Rectifier Using Only Two Active Switches," *IEEE Trans. Ind. Electron.*, vol. 62, no. 5, pp. 2795-2806, May. 2015.

[8] Alireza Abasian, Hosein Farzanehfard and Seyed Madani, "Single Stage Soft Switching AC/DC Converter without Any Extra Switch," *IET Power Electron.*, vol. 7, no. 3, pp. 745-752, Mar. 2014.

[9] Anuwat Jangwanitlert and J. Songboonkaew, "A Soft-Switched AC-DC Symmetrical Boost Converter with Power Factor Correction," *Power Electronics and Drive Systems Conference*, pp. 784-788, 2007.

[10] Jinrong Quian, Qun Zhao and Fred C. Lee, "Single-Stage Single-Switch Power-Factor-Correction AC/DC Converters with DC-Bus Voltage Feedback for Universal Line Applications," *IEEE Trans. on Power Electron.*, vol. 13, no. 6, pp. 1079-1088, Nov. 1998.

[11] Chongming Qian and Keyue-Ma Smedley, "A Topology Survey of Single-Stage Power Factor with a Boost Type Input Current Shaper," *IEEE Trans. on Power Electron.*, vol. 16, no. 3, pp. 360-368, May. 2001.

[12] Oscar Gracia, Jose Cobos, Roberto Prieto, Pedro Alou and Javier Uceda, "Single Phase Power Factor Correction: A Survey," *IEEE Trans. on Power Electron.*, vol. 18, no. 3, pp. 749-755, May. 2003.

[13] Naim Suleyman Ting, Ismail Aksoy and Yakup Sahin, "ZVT-PWM DC–DC Boost Converter with Active Snubber Cell," *IET Power Electron.*, vol. 10, no. 2, pp. 251-260, Feb. 2017.

[14] Naim Suleyman Ting, Yakup Sahin and Ismail Aksoy, "Analysis, Design and Implementation of a Zero-Voltage-Transition Interleaved Boost Converter," *Journal of Power Electron.*, vol. 17, no. 1, pp. 41-55,

Jan. 2017.

[15] Burak Akin and Haci Bodur, "A New Single-Phase Soft-Switching Power Factor Correction Converter," *IEEE Trans. on Power Electron.*, vol. 26, no. 2, pp. 436-443, Feb. 2011.

[16] Chien-Ming Wang, Chang-Hua Lin, Chien-Min Lu and Jyun-Che Li, "Design and Realisation of a Zero-Voltage Transition Pulse-Width Modulation Interleaved Boost Power Factor Correction Converter," *IET Power Electron.*, vol. 8, no. 8, pp. 1542-1551, Aug. 2015.

[17] Gang Yao, Alian Chen and Xiangning He, "Soft Switching Circuit for Interleaved Boost Converters," *IEEE Trans. on Power Electron.*, vol. 22, no. 1, pp. 80-86, Jan. 2007.

[18] Wuhua Li, and X. He, "ZVT Interleaved Boost Converters for High-Efficiency, High Step-Up DC–DC Conversion," *IET Power Electron.*, vol. 1, no. 2, pp. 284-290, Jan. 2007.

[19] Hyun-Lark Do, "Interleaved Boost Converter with a Single Magnetic Component," *IET Power Electron.*, vol. 4, no. 7, pp. 842-849, Apr. 2011.

[20] Yao-Ching Hsieh, Te-Chin Hsueh and Hau-Chen Yen, "An Interleaved Boost Converter with Zero-Voltage Transition," *IEEE Trans. on Power Electron.*, vol. 24, no. 4, pp. 973-978, Apr. 2009.

[21] Wuhua Li and X. He, "High Step-Up Soft Switching Interleaved Boost Converters with Cross-Winding-Coupled Inductors and Reduced Auxiliary Switch Number," *IET Power Electron.*, vol. 2, no. 2, pp. 125-133, Feb. 2009.

[22] Yungtaek Jang and Milan M. Jovanovic, "A Bridgeless PFC Boost Rectifier with Optimized Magnetic Utilization," *IEEE Trans. on Power Electron.*, vol. 24, no. 1, pp. 85-93, Jan. 2009.

[23] Yong Chen, Wen-Ping Dail, Jun Zhou and Eric Hu, "Study and Design of a Novel Three-Phase Bridgeless Boost Power Factor Correction," *IET Power Electron.*, vol. 7, no. 8, pp. 2013-2021, Jul. 2014.

[24] Hsien-Yi Tsai, Tsun-Hsiao Hsia and Dan Chen, "A Novel Soft-Switching Bridgeless Power Factor Correction Circuit," *IEEE Conference on EPE*, pp. 1-10, 2007.

[25] Chien-Ming Wang, "A Novel Zero-Voltage-Switching PWM Boost Rectifier with High Power Factor and Low Conduction Losses," *IEEE Trans. Ind. Electron.*, vol. 52, no. 2, pp. 427-435, Feb. 2005.

[26] Mohammad Reza Mohammadi and Hosein Farzanehfard, "New Family of Zero-Voltage-Transition PWM Bidirectional Converters with Coupled Inductors," *IEEE Trans. Ind. Electron.*, vol. 59, no. 2, pp. 912-919, Feb. 2012.

[27] Haci Bodur and Ahmet Faruk Bakan, "A New ZVT-PWM DC-DC Converter," *IEEE Trans. on Power Electron.*, vol. 17, no. 1, pp. 40-47, Jan. 2002.

[28] Doo-Yong Jung, Young-Hyok Ji, Sang-Hoon Park, Yong-Chae Jung and Chung-Yuen Won "Interleaved Soft-Switching Boost Converter for Photovoltaic Power-Generation System," *IEEE Trans. Power Electron.*, vol. 26, no. 4, pp. 1137-1145, Apr. 2011.

[29] Mohammad Rezvanyvardom, Ehsan Adib and Hosein Farzanehfard, "New Interleaved Zero-Current Switching Pulse-Width Modulation Boost Converter with One Auxiliary Switch," *IET Power Electron.*, vol. 4, no. 9, pp. 979-983, Mar. 2011.

[30] Mohammad Rezvanyvardom, Ehsan Adib, Hosein Farzenahfard and Mehdi Mohammadi, "Analysis, Design and Implementation of Zero-Current Transition Interleaved Boost Converter," *IET Power Electron.*, vol. 5, no. 9, pp. 1804-1812, Jul. 2012.

[31] Yakup Sahin, Naim Suleyman Ting and Ismail Aksoy, "A Single Phase ZVT-ZCT Power Factor Correction Boost Converter," *International Conference on Electrical, Computer and Communication Engineering*, pp. 223-229, Feb. 2016.

[32] Yakup Sahin, "A Novel Soft Switching PWM-PFC AC-DC Boost Converter," *Journal of Electrical Engineering Tech.* vol. 13, no. 1, pp. 256-262, Jan. 2018.

[33] Philip C. Todd, "UC3854 Controlled Power Factor Correction Circuit Design," *UNITRODE Product & Applications Handbook*, 1995-1996.

**Naim Suleyman Ting** received the B.S. degree in Electrical and Electronics Engineering from Erciyes University, Kayseri, Turkey, in 2010; and the M.S. and Ph.D. degrees in Electrical Engineering from Yildiz Technical University, Istanbul, Turkey, in 2013 and 2016, respectively. His research has been concentrated on the areas of soft switching, power factor correction, switching power supplies, high frequency power conversion, and active and passive snubber cells in power electronics. He has published over 30 journal and conference papers in the area of power electronics.